

Dissociation of H_2^+ by Electron Impact: Calculated Angular Distribution*

RICHARD N. ZARE

Joint Institute for Laboratory Astrophysics† and Department of Physics and Astrophysics, University of Colorado, Boulder, Colorado

(Received 25 January 1967)

The angular distribution of products in the electron impact dissociation of H_2^+ has been calculated following closely the Born approximation treatment of E. H. Kerner [Phys. Rev. **92**, 1441 (1953)]. When the translational kinetic energy of separation greatly exceeds the initial rotational energy of the molecule, as is normally the case, the fragments are ejected nearly along the molecular axis. For "axial recoil" the leading term in the differential cross section shows a cosine-squared anisotropy peaked about the momentum-transfer vector, independent of the initial rotational state of the molecule. This is in contrast to the findings of Kerner. The inclusion of higher-order terms in the differential cross section produces interference effects which shift the maximum of the angular distribution away from the momentum transfer vector towards larger angles. However, the contribution of the leading dipole term strongly overshadows the effects of these higher-order multipole terms except in certain cases quite close to threshold. When the angular distribution of products is measured about the electron-beam direction \mathbf{k}_0 , rather than the momentum transfer vector \mathbf{K} , the anisotropy assumes in the dipole limit a simple form proportional to $I_K(\theta) = \cos^2\theta' \cos^2\theta + \frac{1}{2} \sin^2\theta' \sin^2\theta$, where θ' is the angle included between \mathbf{k}_0 and \mathbf{K} . Upon integrating over all possible values of K for a fixed electron-impact energy, the form of the anisotropy is found to be a maximum close to threshold, but is first degraded and then reversed in sense as the bombarding electron energy is increased. In the high-energy limit, however, the angular distribution does not approach a sine-squared anisotropy, but rather a limiting form is asymptotically approached corresponding to an average θ' of about 68° . Comparisons are made with the related experimental studies of G. H. Dunn and L. J. Kieffer [Phys. Rev. **132**, 2109 (1963)] on the dissociative ionization of H_2 .

INTRODUCTION

Calculation of the differential cross section in dissociative electron impact appears quite formidable for the general case, and most attention in the past has been confined to the dissociation of H_2^+ . For this molecule there have been several Born approximation calculations¹⁻⁴ of the total cross section, but only the treatment due to Kerner¹ considers the excitation of different rotational states in treating the $1s\sigma_g \rightarrow 2p\sigma_u$ electronic transition of H_2^+ from the ${}^2\Sigma_g^+$ ground state to the repulsive ${}^2\Sigma_u^+$ state. He finds that the angular distribution will be dominated by the term $P_{J\pm 1, M}(\cos\Theta)$ where Θ is the polar angle measured from the momentum transfer vector \mathbf{K} to the recoiling fragments and where J is the rotational quantum number for the ground state. Thus it is concluded that if the molecule is initially in the rotational ground state ($J=0$), the angular distribution will have mainly a $\cos^2\Theta$ dependence; whereas for the $J=1$ rotational state a spherically symmetric component to the distribution will be important.

Recently Dunn and Kieffer⁵ have studied the angular distribution of fast protons in the dissociative ioniza-

tion of H_2 by electron impact. Near threshold, where dissociative ionization is expected to resemble dissociative excitation,^{5,6} they find a nearly cosine-squared anisotropy. Under their experimental conditions H_2 is predominantly in the $J=1$ rotational state, and the observed angular distribution is in apparent disagreement with the calculations of Kerner.^{1,7}

In the closely related problem of molecular photodissociation, Zare and Herschbach,⁸ using a semiclassical procedure, found for a $\Sigma \rightarrow \Sigma$ transition that the molecule has a preferred orientation for dissociation given by $\cos^2\Theta$, where Θ is now measured from the polarization vector \mathcal{E} . If the molecule dissociates in a time short compared to the rotational period with recoil energy considerably in excess of the molecular rotational energy, as is usually the case,⁹ the direction of departure of the atoms is along the molecular axis (the case of *axial recoil*) and the angular distribution of products will show a corresponding anisotropy.

⁶ G. H. Dunn, Phys. Rev. Letters **8**, 62 (1962).

⁷ J. M. Peek and T. A. Green (Sandia Corporation, Albuquerque, New Mexico) first pointed out this anomalous situation in a conversation with Dr. G. H. Dunn and myself some two years ago. I wish to thank Dr. Green and Dr. Peek for critically reading an early draft of this paper and for bringing to my attention an error involving the correct use of proper boundary conditions for scattering.

⁸ R. N. Zare and D. R. Herschbach, Proc. IEEE **51**, 173 (1963).

⁹ For example in H_2^+ the rotational energy of the molecule is on the order of 0.02 eV; the recoil energy at infinite separation of the fragment partners ranges from about 7 to 13 eV if we consider those vertical transitions from the ground vibrational state to the repulsive potential curve above, which are permitted in the classical limit of the Franck-Condon principle. For further discussion see R. N. Zare and D. R. Herschbach, University of California Radiation Laboratory Report UCRL-10438 (unpublished).

* This research was supported by the Advanced Research Projects Agency (Project DEFENDER), monitored by the U.S. Army Research Office-Durham, under Contract DA-31-124-ARO-D-139.

† Of the National Bureau of Standards and the University of Colorado.

¹ E. H. Kerner, Phys. Rev. **92**, 1441 (1953).

² E. V. Ivash, Phys. Rev. **112**, 155 (1958).

³ R. G. Alsmiller, Jr., Oak Ridge National Laboratory Report ORNL-2766, Oak Ridge, Tennessee, 1959 (unpublished).

⁴ J. M. Peek, (a) Phys. Rev. **134**, A877 (1964); (b) **139**, A1429 (1965); (c) **140**, A11 (1965).

⁵ G. H. Dunn and L. J. Kieffer, Phys. Rev. **132**, 2109 (1963).

Moreover, the effect of the rotational motion of the fragments was explicitly taken into account, and it was shown that the conservation of angular momentum normally forces only a slight blurring in the distribution.

A fully quantum-mechanical description of the photo-dissociation mechanics which gives the quantum correspondence for small J of these semiclassical arguments has been completed.¹⁰ We wish to demonstrate that it follows from an analysis based on Kerner's work that the leading term in the angular distribution varies as $\cos^2\theta$, independent of the rotational state J of the molecule, for the case of nearly axial recoil of the products. Following a presentation of the theory, we examine in detail the effects of including higher-order terms in the differential cross section and the effects of averaging the differential cross section over the allowed orientations and magnitudes of the momentum-transfer vector \mathbf{K} for a fixed electron-bombardment energy. We find the form of the anisotropy integrated over \mathbf{K} is quite similar to the experimental results reported by Dunn and Kieffer⁶ on the analogous problem of the dissociative ionization of H_2 .

THEORY AND DISCUSSION

Born Approximation for the Scattering Amplitude

Consider the collision of a fast electron with an H_2^+ molecule, the internuclear axis of the target system being specified by \mathbf{r} , the internal electronic coordinates by \mathbf{q} , and the distance between the impinging electron and the molecular ion by \mathbf{R} (see Fig. 1). We write the Hamiltonian for the whole system in a coordinate frame in which the center of mass of the complete system is at rest:

$$\mathcal{H} = -(\hbar^2/2\mu)\nabla_{\mathbf{R}}^2 + H^0(\mathbf{q}, \mathbf{r}) + V(\mathbf{q}, \mathbf{r}, \mathbf{R}). \quad (1)$$

Here $\mu = m_e m_{H_2^+} / (m_e + m_{H_2^+})$ is the reduced mass of the total system, where m_e and $m_{H_2^+}$ are the masses of the electron and the hydrogen molecular ion, respectively, $H^0(\mathbf{q}, \mathbf{r})$ is the unperturbed Hamiltonian for the target molecule:

$$H^0(\mathbf{q}, \mathbf{r}) u_i(\mathbf{q}, \mathbf{r}) = E_i u_i(\mathbf{q}, \mathbf{r}), \quad (2)$$

where the u_i are the molecular eigenfunctions of the i th electronic state, and $V(\mathbf{q}, \mathbf{r}, \mathbf{R})$ is the interaction potential between the electron and the H_2^+ ion:

$$V(\mathbf{q}, \mathbf{r}, \mathbf{R}) = -\frac{e^2}{|\mathbf{R} + \frac{1}{2}\mathbf{r}|} - \frac{e^2}{|\mathbf{R} - \frac{1}{2}\mathbf{r}|} + \frac{e^2}{|\mathbf{R} - \mathbf{q}|}. \quad (3)$$

$$c_n(\mathbf{R}) \xrightarrow{R \rightarrow \infty} \exp(ik_n Z) - (4\pi)^{-1} \frac{2\mu \exp(ik_n R)}{\hbar^2 R} \iiint \exp(-i\mathbf{k}_n \cdot \mathbf{R}) u_n^* V \psi d\mathbf{q} d\mathbf{r}. \quad (8)$$

Within the validity of the first Born approximation, we may replace ψ in (8) by the product of an incoming

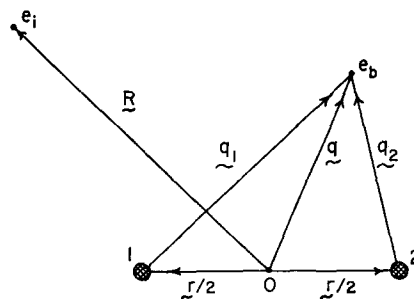


FIG. 1. Coordinate system describing the collision of an incoming electron e_i along \mathbf{R} with a hydrogen molecular ion, Protons 1 and 2 located at $+\mathbf{r}/2$ and $-\mathbf{r}/2$, bound electron e_b at \mathbf{q} . The origin O is at the midpoint of the molecule.

Let the incident electron excite the H_2^+ molecule from the ground state u_0 with energy E_0 to a higher-lying repulsive state u_n with energy E_n in which the incident electron undergoes a momentum change $\hbar\mathbf{K} = \hbar\mathbf{k}_0 - \hbar\mathbf{k}_n$, where $k_i^2 = (2\mu/\hbar^2)(E - E_i)$, $E = (1/2)\mu R^2 + E_0$, and E_i is the energy of the i th target eigenstate. We wish to determine the angular distribution of the dissociation fragments by solving Schrödinger's equation

$$\mathcal{H}\psi = E\psi, \quad (4)$$

for the wavefunction ψ subject to the boundary condition that ψ has the asymptotic form for large R of a plane wave plus scattered outgoing spherical waves:

$$\psi \xrightarrow{R \rightarrow \infty} \exp(i\mathbf{k} \cdot \mathbf{R}) + [\exp(ikR)/R] f_{\mathbf{K}}(\theta, \Phi). \quad (5)$$

Neglecting exchange effects between the incoming and bound electrons, we may expand ψ in terms of the complete set of eigenfunctions $u_i(\mathbf{q}, \mathbf{r})$ belonging to the unperturbed Hamiltonian H^0 :

$$\psi = \sum_i c_i(\mathbf{R}) u_i(\mathbf{q}, \mathbf{r}). \quad (6)$$

By substituting (1) and (6) into (4), multiplying by $u_n^*(\mathbf{q}, \mathbf{r})$, and integrating over all space, we obtain the following inhomogeneous differential equation for the expansion coefficients c_n :

$$(\nabla_{\mathbf{R}}^2 + k_n^2) c_n(\mathbf{R}) = \frac{2\mu}{\hbar^2} \int u_n^* V \psi d\mathbf{q} d\mathbf{r} \quad (7)$$

which, with the aid of Green's functions,¹¹ may be rewritten in integral form:

¹⁰ R. N. Zare, thesis, Harvard University, Cambridge, Mass., 1964 (unpublished); R. N. Zare and D. R. Herschbach, "Mechanics of Molecular Photodissociation" (unpublished).

¹¹ N. F. Mott and H. S. W. Massey, *The Theory of Atomic Collisions* (Clarendon Press, Oxford, England, 1965), 3rd ed., Chap. IV.

plane wave and the wavefunction of the initial unperturbed molecular state:

$$\psi = \exp(i\mathbf{k}_0 \cdot \mathbf{R}) u_0(\mathbf{q}, \mathbf{r}). \quad (9)$$

Thus the Born amplitude for scattering an electron with momentum change $\hbar\mathbf{K}$ for excitation of the target molecule from the state $u_0(\mathbf{q}, \mathbf{r})$ to the state $u_n(\mathbf{q}, \mathbf{r})$ is given by

$$f_K(\Theta, \Phi) = -(4\pi)^{-1} \frac{2\mu}{\hbar^2} \iiint \exp(i\mathbf{K} \cdot \mathbf{R}) u_n^*(\mathbf{q}, \mathbf{r}) V(\mathbf{q}, \mathbf{r}, \mathbf{R}) u_0(\mathbf{q}, \mathbf{r}) d\mathbf{q} d\mathbf{r} d\mathbf{R}, \quad (10)$$

and the differential cross section is given by

$$I_K(\Theta, \Phi) = (k_n/k_0) |f_K(\Theta, \Phi)|^2. \quad (11)$$

Equation (11) is seen to depend on the value of the momentum-transfer vector

$$K^2 - k_0^2 + k_n^2 - 2k_0k_n \cos\omega, \quad (12)$$

where ω is the included angle between \mathbf{k}_0 and \mathbf{k}_n . To obtain the differential cross section of the ejected fragments independent of the angle of the scattered electrons, we must integrate (11) over $\sin\omega d\omega d\phi$ which by (12) is equivalent to $(K/k_0k_n) dK$. We find

$$I = k_0^{-2} \int_{K_{\min}}^{K_{\max}} |f_K|^2 K dK, \quad (13)$$

where the limits of integration range from $K_{\min} = k_0 - k_n$ to $K_{\max} = k_0 + k_n$.

Reduction of the Born Scattering Amplitude

As a result of the orthogonality of the molecular eigenfunctions u_0 and u_n in the electronic coordinate \mathbf{q} , the first two terms $-e^2/|\mathbf{R} \pm \frac{1}{2}\mathbf{r}|$ of the interaction potential (3) cannot contribute to the scattering amplitude (10) and need not be considered further. Making use of the Bethe integral¹²

$$\int \frac{\exp(i\mathbf{K} \cdot \mathbf{a})}{|\mathbf{a} - \mathbf{b}|} d\mathbf{a} = \frac{4\pi}{K^2} \exp(i\mathbf{K} \cdot \mathbf{b}), \quad (14)$$

the integration of the remaining term in (10) $e^2/|\mathbf{R} - \mathbf{q}|$

over $d\mathbf{R}$ is readily performed to yield

$$f_K(\Theta, \Phi) = -\frac{2\mu}{K^2} \iint \exp(i\mathbf{K} \cdot \mathbf{q}) u_n^*(\mathbf{q}, \mathbf{r}) u_0(\mathbf{q}, \mathbf{r}) d\mathbf{q} d\mathbf{r}, \quad (15)$$

where we have adopted for convenience the use of atomic units ($\hbar = m_e = e = 1$) from this point. Further simplification depends on a detailed knowledge of the form of u_0 and u_n . We may write the molecular wavefunction in the Born-Oppenheimer approximation as a product of two terms

$$u_0(\mathbf{q}, \mathbf{r}) = \psi_0(\mathbf{q}, \mathbf{r}) \chi_0(\mathbf{r}), \quad (16a)$$

$$u_n(\mathbf{q}, \mathbf{r}) = \psi_n(\mathbf{q}, \mathbf{r}) \chi_n(\mathbf{r}), \quad (16b)$$

where ψ represents the electronic part of the wavefunction, which is seen to be a parametric function of the internuclear separation \mathbf{r} , and where χ describes the orientation and motion of the nuclei. We take for the lowest-lying bonding and antibonding electronic wavefunctions of H_2^+ , the well-known¹³ linear combination of atomic orbitals

$$\psi_0(\mathbf{q}, \mathbf{r}) = N^{(+)}(\mathbf{r}) [n(q_1) + n(q_2)], \quad (17a)$$

$$\psi_n(\mathbf{q}, \mathbf{r}) = N^{(-)}(\mathbf{r}) [n(q_1) - n(q_2)], \quad (17b)$$

with $n(q) = \pi^{-1/2} e^{-q}$; q_1 and q_2 are radial distances measured from the protons as centers (see Fig. 1); and $N^{(\pm)}(\mathbf{r})$ are normalization factors:

$$N^{(\pm)}(\mathbf{r}) = [2 \pm 2e^{-r} (1 + r + \frac{1}{3}r^2)]^{-1/2}. \quad (18)$$

With this choice of electronic wavefunctions, Eq. (15) becomes

$$f_K(\Theta, \Phi) = -\frac{2\mu}{\pi K^2} \iint \exp(i\mathbf{K} \cdot \mathbf{q}) [\exp(-2q_1) - \exp(-2q_2)] d\mathbf{q} \chi_0(\mathbf{r}) \chi_n^*(\mathbf{r}) N^{(+)}(\mathbf{r}) N^{(-)}(\mathbf{r}) d\mathbf{r}. \quad (19)$$

From Fig. 1 it is apparent that $\mathbf{q} = \mathbf{q}_1 + \frac{1}{2}\mathbf{r} = \mathbf{q}_2 - \frac{1}{2}\mathbf{r}$. Making this change of variables in (19), the integration over $d\mathbf{q}$ may be carried out in a straightforward manner to give

$$f_K(\Theta, \Phi) = -\frac{64\mu i}{K^2(4+K^2)^2} \int \sin(\frac{1}{2}\mathbf{K} \cdot \mathbf{r}) N^{(+)}(\mathbf{r}) N^{(-)}(\mathbf{r}) \chi_n^*(\mathbf{r}) \chi_0(\mathbf{r}) d\mathbf{r}. \quad (20)$$

¹² H. A. Bethe, *Ann. Physik* 5, 325 (1930).

¹³ J. C. Slater, *Electronic Structure of Molecules* (McGraw-Hill Book Co., New York, 1963), Chaps. 1 and 2. Born cross sections calculated with these approximate wavefunctions compare favorably with results obtained using exact H_2^+ electronic wavefunctions [see Ref. 3 and Ref. 4(b)].

The nuclear wavefunctions χ_0 and χ_n appearing in (20) are eigenstates of the Hamiltonians for the nuclear motions in the initial and final states:

$$[-(1/2\mu')\nabla_r^2 + V_{0,n}]\chi_{0,n} = E_{0,n}\chi_{0,n}, \quad (21)$$

where $V_{0,n}$ are the effective nuclear potential energy curves of these states and μ' is the reduced mass of the molecule. The radial parts of $\chi_{0,n}$, which describe the vibrational motion of the nuclei, satisfy the radial Schrödinger equation

$$\left[-\frac{1}{2\mu' r^2} \frac{d}{dr} \left(r^2 \frac{d}{dr} \right) + V_{0,n}(r) + \frac{J(J+1)}{2\mu' r^2} \right] R_{J^0,n} = E_{0,n} R_{J^0,n}, \quad (22)$$

and the angular parts, which describe the orientation of the nuclei, can be described in terms of spherical harmonics.

For the bound-state nuclear wavefunction, we choose a definite vibration-rotation (v, J) state

$$\chi_0(\mathbf{r}) = R_{vJ^0}(r) Y_{JM}(\theta, \phi), \quad (23)$$

where we take the axis of quantization to lie along \mathbf{K} . Equation (23) corresponds to a stationary state of the molecule with definite values of the energy, angular momentum, and projection thereof.

The continuum nuclear wavefunction must be chosen to satisfy the proper boundary conditions for scattering, namely that χ_n^* has the asymptotic form of an *outgoing* plane wave plus outgoing spherical waves:

$$\chi_n^*(\mathbf{r}) \xrightarrow[r \rightarrow \infty]{} A \{ \exp(-i\boldsymbol{\kappa} \cdot \mathbf{r}) + f(\theta) [\exp(i\kappa r)/r] \}, \quad (24)$$

where $\boldsymbol{\kappa}$ is the propagation vector and \mathbf{r} the position vector.¹⁴ For dissociative excitation $\boldsymbol{\kappa}$ points along the final recoil direction of the fragments and \mathbf{r} coincides with the molecular axis, as is pictured in Fig. 2. Then

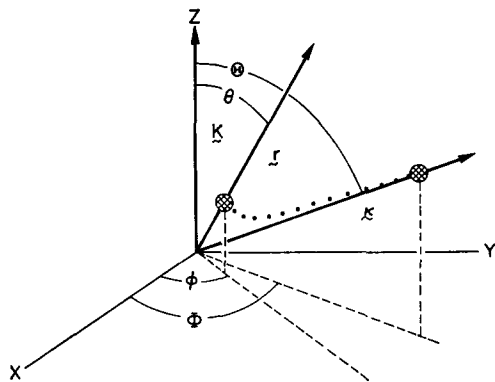


FIG. 2. The recoiling atom (the classical trajectory of which is indicated by the dotted line) is scattered by the repulsive molecular potential. The quantization axis \mathbf{K} is along the Z axis; the propagation vector $\boldsymbol{\kappa}$ is along the asymptote of the recoiling atoms; and the position vector \mathbf{r} coincides with the molecular axis. For molecular dissociation the recoiling fragments generally have considerable kinetic energy so that $\boldsymbol{\kappa}$ and \mathbf{r} nearly coincide throughout.

¹⁴This choice for the form of the continuum wavefunction ensures that the plane-wave and spherical-wave parts of (24) interfere in such a way that $\chi_n^*(r)$ corresponds to an outgoing radial flux. For further discussion see G. Breit and H. A. Bethe, Phys. Rev. **93**, 888 (1954).

the continuum wavefunction may be put in a form similar to Eq. (23):

$$\chi_n^*(\mathbf{r}) = \sum_{J'} (2J'+1) (-i)^{J'} \times \exp(i\delta_{J'}) R_{J'^n}(r) P_{J'}(\hat{\boldsymbol{\kappa}} \cdot \hat{\mathbf{r}}). \quad (25)$$

Here $\chi_n^*(\mathbf{r})$, built up from radial wavefunctions $R_{J'^n}(r)$ which satisfy Eq. (22), has the form at large separation of a sine wave:

$$\sin[\kappa r - \frac{1}{2}(J'\pi) + \delta_{J'}]/\kappa r, \quad (26)$$

with phase shift $\delta_{J'}$; and the angles in (25) are measured between the unit vectors $\hat{\boldsymbol{\kappa}}$ and $\hat{\mathbf{r}}$ and are not the same angles as in Eq. (23). Moreover, by using the addition theorem for spherical harmonics, we may recast $P_{J'}(\hat{\boldsymbol{\kappa}} \cdot \hat{\mathbf{r}})$ in the form

$$P_{J'}(\hat{\boldsymbol{\kappa}} \cdot \hat{\mathbf{r}}) = \frac{4\pi}{2J'+1} \sum_{M'=-J'}^{J'} Y_{J'M'}^*(\theta, \phi) Y_{J'M'}(\Theta, \Phi), \quad (27)$$

where the angles (θ, ϕ) give the orientation of the molecular axis with respect to \mathbf{K} and where (Θ, Φ) locate the direction of the recoiling atoms at large separation (Fig. 2) with respect to \mathbf{K} , so that

$$\chi_n^*(\mathbf{r}) = 4\pi \sum_{J'} \sum_{M'=-J'}^{J'} (-i)^{J'} \times \exp(i\delta_{J'}) R_{J'^n}(r) Y_{J'M'}^*(\theta, \phi) Y_{J'M'}(\Theta, \Phi). \quad (28)$$

The continuum nuclear wavefunction given by Eq. (28) corresponds to a stationary state of the molecule with a definite value of the energy $E = \kappa^2/2\mu$, but not to a definite state of angular momentum.

The term $\sin(\frac{1}{2}\mathbf{K} \cdot \mathbf{r})$ appearing in Eq. (20) also may be expressed in terms of the angles defined in Fig. 2. With the help of the expansion of a plane wave in terms of Legendre polynomials, we find that

$$\sin(\frac{1}{2}\mathbf{K} \cdot \mathbf{r}) = (2i)^{-1} \sum_{l=0}^{\infty} (2l+1) i^l \times [j_l(\frac{1}{2}Kr) - (-1)^l j_l(\frac{1}{2}Kr)] P_l(\cos \theta), \quad (29)$$

where the $j_l(\frac{1}{2}Kr)$ are spherical Bessel functions. It is apparent that the $l=1$ term in (29) strongly dominates for small angle scattering ($K \rightarrow 0$) where $j_l(\frac{1}{2}Kr)$ may be replaced by $[l!/(2l+1)!](Kr)^l$. We note that Eq.

(29) resembles a multipole-moment expansion, the first term ($l=1$) having the angular form of the dipole moment, the second term ($l=3$) that of an octopole moment, etc. All even values of l in Eq. (29) vanish.

Upon replacing in Eq. (20) χ_0 by Eq. (23), χ_n^* by Eq. (28) and $\sin(\frac{1}{2}\mathbf{K}\cdot\mathbf{r})$ by the leading term in Eq. (29), we find that the Born scattering amplitude may

be put into the simple form

$$f_K(\Theta, \Phi) \sim [K(4+K^2)]^{-2} \sum_{J'} \sum_{M'} \mathcal{R}_{J'} \mathcal{Q}_{J'} Y_{J'M'}(\Theta, \Phi), \quad (30)$$

where we omit all numerical constants which do not affect the form of the angular distribution. Here

$$\mathcal{R}_{J'} = (-i)^{J'} \exp(i\delta_{J'}) \int N^{(+)}(\mathbf{r}) N^{(-)}(\mathbf{r}) R_{J'}^n(\mathbf{r}) j_1(\frac{1}{2}Kr) R_{vJ'}^0(\mathbf{r}) r^2 dr \quad (31)$$

is a radial term governing the band strength of the transition, and

$$\mathcal{Q}_{J'} = (\frac{4}{3}\pi)^{1/2} \int Y_{J'M'}^*(\theta, \phi) Y_{10}(\theta, \phi) Y_{JM}(\theta, \phi) \sin\theta \, d\theta \, d\phi \quad (32)$$

is an angular term giving the rotational line strength factor for a specific $JM \rightarrow J'M'$ transition. Equation (32) reduces¹⁶ to

$$\mathcal{Q}_{J'} = [(2J+1)/(2J'+1)]^{1/2} C(J1J'; 00) C(J1J'; MO), \quad (33)$$

where the C 's are Clebsch-Gordan coefficients. The differential cross section is then obtained [see Eq. (11)] by squaring the scattering amplitude given by Eq. (30) and summing over all the indistinguishable M' sublevels¹⁶ of the initial state:

$$I_K(\Theta, \Phi) = F(K) \sum_M \left| \sum_{J'} \sum_{M'} \mathcal{R}_{J'} [(2J+1)/(2J'+1)]^{1/2} C(J1J'; 00) C(J1J'; MO) Y_{J'M'}(\Theta, \Phi) \right|^2, \quad (34)$$

where the factor $F(K) = k_0^{-1} k_n [K(4+K^2)]^{-4}$.

The "Axial-Recoil" Approximation

The detailed evaluation of the form of the scattering cross section requires a knowledge of the variation of the radial term $\mathcal{R}_{J'}$ with J' over the limited range of J' ($J'=J\pm 1$) for which the sum in Eq. (34) does not vanish. Fortunately, a powerful simplification is possible when the molecular transition induced by electron impact is to a strongly sloping portion of the repulsive potential curve, as is normally the circumstance.⁹ Then the fragments depart from each other with considerable kinetic energy compared to their rotational energy and are thus ejected in the direction in which the molecular axis was pointing at the time of dissociative electron impact (axial recoil). In this case the scattering is almost classical and the phase shift $\delta_{J'}$ appearing in Eq. (31) may be estimated semiclassically to good approximation. In the Appendix we show that for large recoil energies

$$\delta_{J'} = \frac{1}{2}(J'\pi) - C, \quad (35)$$

where C is a constant to order $[(J'+\frac{1}{2})/kr]^2$. Then the factor $(-i)^{J'} \exp(i\delta_{J'})$ appearing in (31) equals $\exp(-iC)$, which is independent of J' to high accuracy. Furthermore, under these conditions the radial continuum wavefunction $R_{J'}^n(\mathbf{r})$ is chiefly determined by the nuclear potential term $V_n(\mathbf{r})$ rather than the centrifugal potential term $J'(J'+1)/2\mu r^2$ appearing in Eq. (22), and consequently is only weakly dependent on J' through the latter potential term which causes a small correction in the form of $R_{J'}^n(\mathbf{r})$ due to rotational distortion of the molecule.¹⁷ Thus for nearly axial recoil of the fragments, the radial term $\mathcal{R}_{J'}$ is roughly a constant over the rotational structure and may be taken outside the sum over J' and M' occurring in (34).

With this approximation, which is exact for purely axial recoil, the sum over J' and M' is readily performed

¹⁶ Here we assume that the molecular ensemble is randomly oriented and has not been prepared with unequal M state populations.

¹⁷ For a discussion of vibration-rotation interaction in diatomic molecules see for example (a) T. C. James, thesis, Harvard University, 1960 (unpublished); (b) J. K. Cashion, *J. Mol. Spectry.* **10**, 182 (1963); *J. Chem. Phys.* **41**, 3988 (1964).

¹⁵ M. E. Rose, *Elementary Theory of Angular Momentum* (John Wiley & Sons, Inc., New York, 1957).

by reference to a simplified form of the Clebsch–Gordan series¹⁵:

$$\sum_{J'} \sum_M [(2J+1)/(2J'+1)]^{1/2} C(J1J'; 00) C(J1J'; Mm) Y_{J'M'}(\Theta, \Phi) = Y_{1m}(\Theta, \Phi) Y_{JM}(\Theta, \Phi), \quad (36)$$

and we find the Born scattering cross section reduces to

$$\begin{aligned} I_K(\Theta, \Phi) &= F(K) \left| \mathcal{R} \right|^2 \sum_M Y_{10}(\Theta, \Phi) Y_{J'M'}(\Theta, \Phi) \left|^2 \right. \\ &= F(K) \left| \mathcal{R} \right|^2 \cos^2\Theta. \end{aligned} \quad (37)$$

Equation (37) is independent of J' and J .

These conclusions are for nearly axial recoil of the dissociation fragments. When this approximation ($\kappa \gg J' + \frac{1}{2}$) is no longer applicable, such as close to the threshold for dissociation or for the dissociation of very high excited rotational levels, we must evaluate the terms in (34) separately. This task appears quite formidable although certainly tractable. However, from semiclassical considerations it has been shown elsewhere⁸ that the effect of this additional rotational mo-

mentum of the molecule is to suppress the sharp features of the angular distribution at first, and in the extreme case where the fragments are ejected at right angles to the initial direction of the molecular axis (transverse recoil), to reverse fully the form of the anisotropy. Furthermore, we have shown before that this rotational “blurring” of the angular distribution is normally only a small effect, so that the approximation of axial recoil holds for most examples encountered in the dissociation of molecules.

The same qualitative conclusions can be reached from purely quantum considerations. Starting from Eq. (34) and substituting algebraic expressions¹⁵ for the Clebsch–Gordan coefficients, the differential cross section may be shown to have the explicit form

$$\begin{aligned} I_K(\Theta, \Phi) &= F(K) \sum_M \left| \left[\frac{(J+1)^2 - M^2}{(2J+1)(2J+3)} \right]^{1/2} \mathcal{R}_{J+1} Y_{J+1M}(\Theta, \Phi) \right. \\ &\quad \left. + \left[\frac{J^2 - M^2}{(2J+1)(2J-1)} \right]^{1/2} \mathcal{R}_{J-1} Y_{J-1M}(\Theta, \Phi) \right|^2. \end{aligned} \quad (38)$$

The sum over M in (38) may be readily carried out with the help of the following algebraic identities¹⁸:

$$\sum_m |Y_{lm}(\theta, \phi)|^2 = (2l+1)/4\pi, \quad (39a)$$

$$\sum_m m^2 |Y_{lm}(\theta, \phi)|^2 = [l(l+1)(2l+1)/8\pi] \sin^2\theta, \quad (39b)$$

and

$$\begin{aligned} \sum_m \left[\frac{(l+m+1)(l+m)(l-m+1)(l-m)}{(2l+1)(2l+3)(2l-1)(2l+1)} \right]^{1/2} Y_{l+1m}^*(\theta, \phi) Y_{l-1m}(\theta, \phi) \\ = \sum_m \left[\frac{(l+m+1)(l+m)(l-m+1)(l-m)}{(2l+1)(2l+3)(2l-1)(2l+1)} \right]^{1/2} Y_{l+1m}(\theta, \phi) Y_{l-1m}^*(\theta, \phi) \\ = \frac{l(l+1)}{8\pi(2l+1)} (3 \cos^2\theta - 1). \end{aligned} \quad (39c)$$

The differential cross section is then found to be of the form

$$I(\Theta, \Phi) \sim a + b \cos^2\Theta, \quad (40)$$

where

$$a = J(J+1) [|\mathcal{R}_{J+1}|^2 + |\mathcal{R}_{J-1}|^2 - (\mathcal{R}_{J+1}^* \mathcal{R}_{J-1} + \mathcal{R}_{J+1} \mathcal{R}_{J-1}^*)], \quad (41a)$$

and

$$b = (J+1)(J+2) |\mathcal{R}_{J+1}|^2 + J(J-1) |\mathcal{R}_{J-1}|^2 + 3J(J+1) (\mathcal{R}_{J+1}^* \mathcal{R}_{J-1} + \mathcal{R}_{J+1} \mathcal{R}_{J-1}^*). \quad (41b)$$

¹⁸ Equation (39a) is a consequence of the closure relations for the spherical harmonics. Equation (39b), which is derived in Ref. 10, can be found from Eq. (27) by differentiating twice with respect to ϕ and then setting $\Theta = \theta$ and $\Phi = \phi = 0$. Equation (39c) may be derived from Eq. (39b) by squaring the identity

$$\cos\Theta Y_{lm}(\Theta, \Phi) = [(l+m+1)(l-m+1)/(2l+1)(2l+3)]^{1/2} Y_{l+1m}(\Theta, \Phi) + [(l+m)(l-m)/(2l-1)(2l+1)]^{1/2} Y_{l-1m}(\Theta, \Phi).$$

The ratio a/b provides a convenient measure of the degree of anisotropy present in $I(\Theta, \Phi)$. For purely axial recoil, $\mathcal{R}_{J+1}=\mathcal{R}_{J-1}$, $a/b=0$, and the angular distribution is strictly proportional¹⁹ to $\cos^2\Theta$. As we relax the equality between \mathcal{R}_{J+1} and \mathcal{R}_{J-1} , the anisotropy of the distribution is diminished but is rather insensitive to small differences between \mathcal{R}_{J+1} and \mathcal{R}_{J-1} when these two radial terms are of comparable magnitude. For example if $\mathcal{R}_{J+1}=0.9 \mathcal{R}_{J-1}$, $a/b=0.01$, and the angular distribution still exhibits effectively a $\cos^2\Theta$ anisotropy for most practical purposes. In the extreme case of transverse recoil, it can be shown²⁰ that as the dissociation threshold is approached, the phase shift δ_J goes to zero as κ tends to zero. Then $\mathcal{R}_{J+1}=-\mathcal{R}_{J-1}$, the ratio $a/b=-1$, and the anisotropy of the angular distribution of products possesses a $\sin^2\Theta$ dependence, in agreement with the semiclassical arguments we have previously advanced. Henceforth we restrict our attention to those molecular dissociation processes sufficiently far from threshold that we can disregard the residual effects of rotational motion on the trajectories of the fragments.

Interference Terms in the Differential Scattering Cross Section

Using the same arguments as above, we may include the higher-order terms of the plane-wave expansion (29) in (34). The resulting differential cross section is given by

$$I_K(\Theta, \Phi) = F(K) \left| \sum_{l=1,3,5}^{\infty} \alpha_l P_l(\cos\Theta) \right|^2, \quad (42)$$

where the coefficients α_l , within a constant phase factor, are proportional to

$$\alpha_l = (i)^l (2l+1) \times \int N^{(+)}(\mathbf{r}) N^{(-)}(\mathbf{r}) R_{J^+}(\mathbf{r}) j_l(\frac{1}{2}K\mathbf{r}) R_{J^0}(\mathbf{r}) r^2 d\mathbf{r}. \quad (43)$$

From Eq. (42) it is apparent that the differential cross section $I(\Theta, \Phi)$ (a) possesses cylindrical symmetry²¹ about \mathbf{K} , being independent of Φ ; (b) possesses forward-backward symmetry about a plane through the scattering center at right angles to \mathbf{K} , since the cross section is an even function of $\cos\Theta$; and (c) vanishes at $\Theta=\pi/2$. The inclusion of higher-order terms in (42) corresponds to the scattering of higher-order partial waves. Although the $\cos^2\Theta$ term is normally the largest term in (42), the presence of the other terms which enter with different powers of i gives rise to interference effects.

¹⁹ For the special case in which the molecule has no rotational angular momentum ($J=0$), Eqs. (41a) and (41b) show that a/b is always zero, as would be expected on classical grounds.

²⁰ Reference 11, Chap. II, Sec. 9.

²¹ For a general treatment of symmetries in the angular distribution of products in electron impact see Ref. 6.

To estimate the relative importance of these additional terms, we must evaluate the α_l coefficients. We choose a specific example pertinent to the electron-impact dissociation of H_2^+ , namely, a dissociative transition in which the molecule makes a vertical jump from the center of the lowest vibrational state ($v=0$) to the repulsive potential curve 11.4 eV directly above. The fragment partners then separate from each other with about 8.75-eV excess kinetic energy divided equally between the recoil partners. The evaluation of α_l requires accurate repulsive and bound-state radial wavefunctions which can be obtained by a numerical solution of Eq. (22). However, to avoid an elaborate calculation, we use a popular method first introduced by Winans and Stueckelberg.²² The upper-state repulsive eigenfunction is replaced by a properly normalized delta function $N\delta(\mathbf{r}-\mathbf{r}_0)$ which is different from zero only at the classical turning point, where \mathbf{r}_0 is taken to be the internuclear equilibrium distance, $r_0 \simeq 2a_0$, for the H_2^+ ground state.²³ Results obtained in this manner differ only very slightly from those obtained with correct repulsive wavefunctions, as Coolidge, James, and Present,²⁴ and Kieffer and Dunn²⁵ have shown in detail. The differential cross section then assumes the simple form

$$I_K(\Theta, \Phi) = F(K) \times \left| \sum_{l=1,3,5}^{\infty} (i)^l (2l+1) j_l(\frac{1}{2}K\mathbf{r}_0) P_l(\cos\Theta) \right|^2, \quad (44)$$

where we have dropped all angle-independent and K -independent factors.

Equation (44) has been evaluated numerically, and the results are presented in Fig. 3 for different values of the momentum transfer vector \mathbf{K} (in atomic units of a_0^{-1}). Figure 3 shows that the differential cross section distorts from a cosine-squared dependence on Θ at small values of K to an eccentric-shaped distribution. The maximum in the distribution moves away from the poles ($\Theta=0, \pi$) towards the equator ($\Theta=\pi/2$) with increasing momentum-transfer change. These results hold for as large K as we have investigated the form of the scattering cross section ($K=2.5 a_0^{-1}$). The same behavior was reported previously by Peek,²⁶ who used the exact electronic wavefunctions for the H_2^+ mole-

²² J. G. Winans and E. C. G. Stueckelberg, Proc. Natl. Acad. Sci. (U.S.) **14**, 867 (1928).

²³ From what follows it will become apparent that the value chosen for \mathbf{r}_0 in general only slightly affects the form of the cross section. However, this will not be true if the energy spread of the electron beam is wide and/or several vibrational states can contribute to the dissociation process. Then we must take into account not only the changing magnitude of $K\mathbf{r}$, but also the fact that the electronic transition moment is a strong function of internuclear separation, as has been well verified by both calculation and experiment (see the literature citations given in Ref. 32).

²⁴ A. S. Coolidge, H. M. James, and R. D. Present, J. Chem. Phys. **4**, 193 (1936).

²⁵ L. J. Kieffer and G. H. Dunn, "Dissociative Ionization of H_2 and D_2 ," Phys. Rev. (to be published).

²⁶ See Fig. 3 of Ref. 4(a).

cule. We show in the next section, however, that the form of the differential cross section usually is strongly dominated by small values of K less than $1.0 a_0^{-1}$, so that the higher-multipole interference terms are masked by the leading dipole term and make only a small contribution to the over-all shape of the angular distribution. An exception to this can occur close to threshold where K and k_0 are comparable in magnitude.²⁷ Provided $k_0 \geq 1.5 a_0^{-1}$, these interference effects are predicted to strikingly alter the expected $\cos^2\theta$ dependence of the angular distribution.

The Average of the Fragment Angular Distribution Over All Electron-Scattering Angles

We have calculated so far the form of the angular distribution $I_K(\theta, \Phi)$ of the dissociation fragments for a fixed magnitude of the momentum transfer vector \mathbf{K} , where the angles θ, Φ are measured about \mathbf{K} as the polar axis. However, it is quite difficult experimentally to determine simultaneously both the distribution of the fragments and the scattering angles of the electrons. Rather than making such coincidence measurements, it is customary to observe the angular distribution of products, without regard to the scattered electrons. The direction of the electron beam \mathbf{k}_0 then serves as a convenient reference coordinate system for reporting the form of the angular distribution. In order to present our calculated angular distributions in a manner which can be readily compared with experiment, we must average $I_K(\theta, \Phi)$ over all possible orientations and magnitudes of \mathbf{K} .

We begin by discussing the transformation of the scattering cross section measured in the "momentum-transfer" frame to the "electron-beam" frame. From physical considerations it is evident that the flux of particles does not depend on the choice of the coordinate system. Thus the number of particles emitted into corresponding solid angle elements must be the same in the \mathbf{K} and \mathbf{k}_0 frames, and therefore the differential cross sections are related by

$$I_K(\theta, \Phi) \sin\theta d\theta d\Phi = I_K(\theta, \phi) \sin\theta d\theta d\phi. \quad (45)$$

Accordingly, the transformation of angular distributions is given by

$$I_K(\theta, \phi) = J(\theta, \Phi) I_K(\theta, \Phi), \quad (46)$$

where $J(\theta, \Phi)$ is the Jacobian of the transformation

$$J(\theta, \Phi) = \begin{vmatrix} \partial \cos\theta / \partial \cos\theta & \partial \cos\theta / \partial \phi \\ \partial \Phi / \partial \cos\theta & \partial \Phi / \partial \phi \end{vmatrix}, \quad (47)$$

giving the ratio of the infinitesimal solid angle elements

²⁷ This threshold, corresponding to just sufficient electron beam energy to cause a molecular transition to a certain point on the upper state repulsive curve, is to be clearly distinguished from the dissociation threshold, corresponding to the separation of the fragments with "zero" kinetic energy discussed in the previous section.

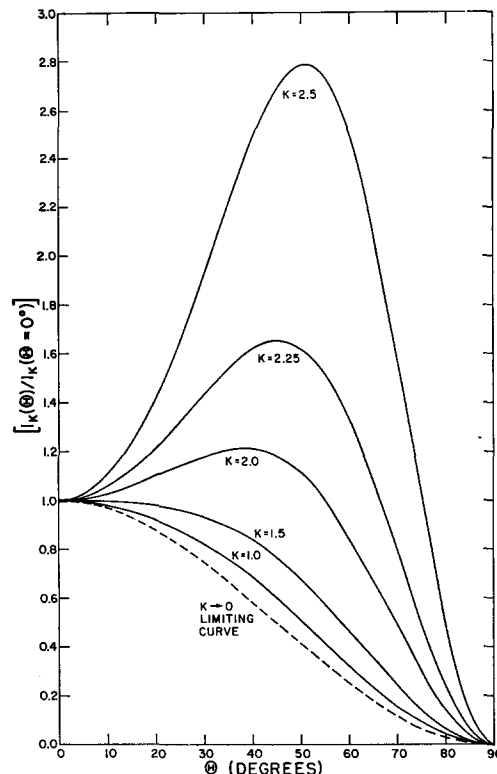


FIG. 3. Variation of the differential cross section $I_K(\theta, \Phi)$ with increasing momentum transfer K for the dissociation of H_2^+ to produce 4.38 eV protons, corresponding to a vertical transition from the midpoint ($r_0 \approx 2a_0$) of the vibrational ground state ($v=0$) to the repulsive-potential curve above. The units of K are reciprocal Bohr radii (a_0^{-1}).

in the two respective coordinate systems:

$$J(\theta, \Phi) = \sin\theta d\theta d\Phi / \sin\theta d\theta d\phi. \quad (48)$$

Figure 4 defines the relevant scattering angles (θ, Φ) and (θ, ϕ) where θ' is the included angle between \mathbf{k}_0 and \mathbf{K} . We have chosen the X axis of the \mathbf{k}_0 frame in Fig. 4 so that $\Phi=0^\circ$. Then the scattering angles are related to each other by

$$\cos\theta = \cos\theta \cos\theta' + \sin\theta \sin\theta' \cos\phi \quad (49a)$$

and

$$\Phi = \sin^{-1}(\sin\theta \sin\phi / \sin\theta'). \quad (49b)$$

Figure 4 shows that the \mathbf{K} and \mathbf{k}_0 frames may be transformed into each other through a simple rotation by θ' about the (Y, y) axis. Consequently there is no distortion in their solid-angle elements, and it is apparent that the Jacobian factor is unity in Eq. (46). The same conclusion may also be readily reached by evaluating the expression for the Jacobian in Eq. (47) with the help of Eqs. (49a) and (49b).

The angular distribution $I_K(\theta, \Phi)$ has previously been shown to be cylindrically symmetric about \mathbf{K} , so that points of equal flux of scattered particles lie on a cone with apex half-angle θ about \mathbf{K} . We may consider in turn \mathbf{K} to rotate about \mathbf{k}_0 on the surface of a

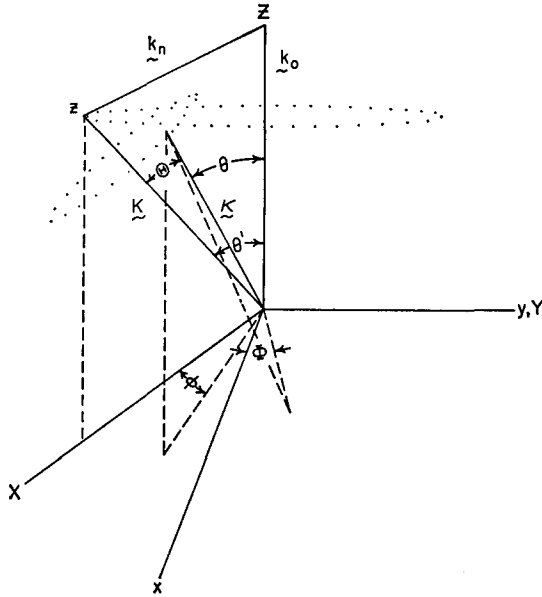


FIG. 4. Relation between scattering angles in the electron beam and momentum transfer coordinate system. The location of the X and Y axes in the \mathbf{k}_0 frame is chosen so that \mathbf{K} lies in the XZ plane and the y axes of the \mathbf{k}_0 and \mathbf{K} frames coincide (line of nodes). Fragments ejected along κ are described by the polar angles (θ, ϕ) and (Θ, Φ) in the two respective frames.

cone with apex half-angle being given by θ' (see Fig. 4). Thus the angular distribution $I_K(\theta, \phi)$ must also be cylindrically asymmetric about \mathbf{k}_0 . In order to take into account all possible orientations of \mathbf{K} with respect to \mathbf{k}_0 , we must integrate over the azimuthal angle ϕ whatever relationships we deduce for the choice of coordinates pictured in Fig. 4.

In particular we find for the angular distribution in the \mathbf{k}_0 frame for a fixed value but an arbitrary direction of \mathbf{K} :

$$I_K(\theta, \phi) = F(K) \left| \sum_{l=1,3,5}^{\infty} (i)^l (2l+1) j_l(\frac{1}{2}K r_0) \times \left[(2\pi)^{-1} \int_0^{2\pi} P_l(\cos\theta \cos\theta' + \sin\theta \sin\theta' \cos\phi) d\phi \right] \right|^2, \tag{50}$$

which in the dipole limit ($l=1$) takes the form²⁸

$$I_K(\theta, \phi) \sim \cos^2\theta \cos^2\theta' + \frac{1}{2} \sin^2\theta \sin^2\theta'. \tag{51}$$

From Eq. (51) we can assess how the differential cross section, measured about the electron-beam direction, varies with the angle that \mathbf{K} makes with \mathbf{k}_0 . In Fig. 5 we present polar plots of $I_K(\theta, \phi)$ for various equally spaced values of θ' . From these plots it is apparent that with increasing θ' the distribution smoothly distorts from a $\cos^2\theta$ dependence for \mathbf{K} parallel to \mathbf{k}_0 to a $\sin^2\theta$ dependence for \mathbf{K} perpendicular to \mathbf{k}_0 . Some of the properties of $I_K(\theta, \phi)$ are readily discussed in

²⁸ Equation (51) is the same as Eq. (30) in Ref. 8.

terms of the so-called "magic angle" of 54.7° , first introduced by Van Vleck²⁹ in his treatment of polarized emission from atoms. For example Fig. 5 shows that for $\theta' < \theta'_{\text{magic}}$, the maximum in the angular distribution occurs along \mathbf{k}_0 in the forward and backward directions; for $\theta' = \theta'_{\text{magic}}$, the distribution is isotropic; and for $\theta' > \theta'_{\text{magic}}$, the distribution peaks in a plane perpendicular to \mathbf{k}_0 . We also note if the fragment distribution is viewed in Fig. 5 along the "magic angle" $\theta = 54.7^\circ$, the flux of particles is independent of the form of the anisotropy.

By reference to Eq. (13) the angular distribution $I(\theta, \phi)$ averaged over all directions and magnitudes of \mathbf{K} is readily found from Eq. (50):

$$I(\theta, \phi) = \frac{1}{k_0^2} \int_{K_{\text{min}}}^{K_{\text{max}}} \frac{dK}{K^3(4+K^2)^4} \left| \sum_{l=1,3,5}^{\infty} (i)^l (2l+1) j_l(\frac{1}{2}K r_0) \times \left[(2\pi)^{-1} \int_0^{2\pi} P_l(\cos\theta \cos\theta' + \sin\theta \sin\theta' \cos\phi) d\phi \right] \right|^2 \tag{52}$$

where the dependence of θ' on \mathbf{K} is given explicitly by

$$\cos\theta' = (K^2 + k_0^2 - k_n^2) / 2k_0 K. \tag{53}$$

We wish to discuss the behavior of $I(\theta, \phi)$ with electron bombardment energy E_0 in terms of two limiting cases: (1) close to threshold, where θ' is restricted to small angles, as shown in Fig. 6(a); and (2) far from threshold at high electron-beam energies where for small momentum transfer θ' approaches 90° , as shown in Fig. 6(b). It is tempting to suppose that we can interpret the variation of $I(\theta, \phi)$ with increasing electron-

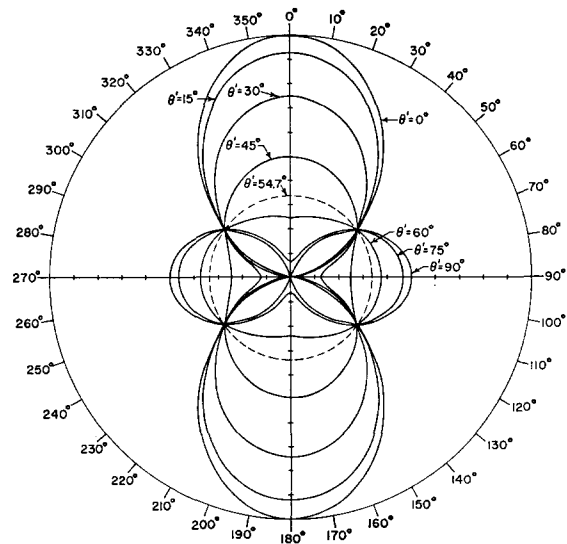


FIG. 5. Behavior of $I_K(\theta, \phi)$ as a function of θ' , the included angle between \mathbf{K} and \mathbf{k}_0 . All cross sections have been normalized to the same flux.

²⁹ J. H. Van Vleck, Proc. Natl. Acad. Sci. (U.S.) 11, 612 (1925).

bombardment energy as a gradual transition between these two limiting cases. Thus we might expect that the anisotropy in the angular distribution of dissociation products would be at a maximum at threshold, but will be first suppressed, then reversed in sense and finally tend to a $\sin^2\theta$ distribution if the electron bombardment energy is increased sufficiently.

We are in a position to put these intuitive motions on a quantitative basis by numerically evaluating Eq. (52). The results are pictured in Fig. 7, which shows $I(\theta, \phi)$ as a function of the electron beam energy E_0 , where the distribution is normalized to unity at $\theta=90^\circ$ and 270° . On examining Fig. 7 we find our expectations are fulfilled by and large, but with the remarkable exception that $I(\theta, \phi)$ instead of showing a $\sin^2\theta$ distribution in the limit of high energy, approaches asymptotically a form which is only slightly peaked in a plane at right angles to \mathbf{k}_0 . The explanation for this seemingly

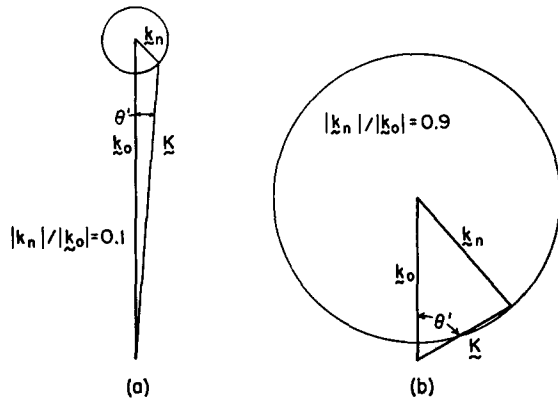


FIG. 6. The relationship between the vectors \mathbf{k}_0 , \mathbf{k}_n , and \mathbf{K} and the angle θ' : (a) close to threshold; (b) far from threshold. The values of θ' range from 0° to $\sin^{-1}[|\mathbf{k}_n|/|\mathbf{k}_0|]$ which is reached when K is tangent to the circle of possible orientations of \mathbf{k}_n shown above.

paradoxical behavior is that the dependence of $I(\theta, \phi)$ on K weights strongly small values of K close to K_{\min} , the lower limit of the integration in Eq. (52). As $K \rightarrow K_{\min}$, $\theta' \rightarrow 0^\circ$ in both limiting cases shown in Fig. 6. Consequently small angles of θ' contribute heavily to the form of $I(\theta, \phi)$.

It might be wondered whether the $\sin^2\theta$ limiting form would be reached, provided we were to consider still higher energies³⁰ than shown in Fig. 7. However, this is not the case, as can be demonstrated in the following manner. Let us calculate the fractional contribution to the total integral made by those values of θ' that are less than or equal to θ'_{magic} . As we have previously noted (see Fig. 5), such values of $\theta' \leq \theta'_{\text{magic}}$, corresponding to the limits of integration from K_{\min}

³⁰ The largest electron energy considered in Fig. 7, $E_0=3$ kV, corresponds to over 250 times the threshold energy for producing 4.38-eV protons. At this energy $|\mathbf{k}_0|=1.482a_0^{-1}$ and $|\mathbf{k}_n|=1.479a_0^{-1}$, so that $\theta'_{\text{max}}=86.3^\circ$.

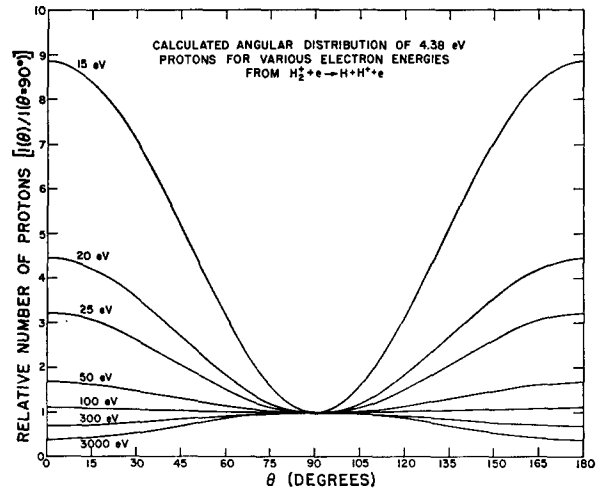


FIG. 7. Variation of the form of the differential cross section $I(\theta, \phi)$ with electron-bombardment energy E_0 . The angular distribution, which is calculated from (52) with $r_0=2a_0$ and for a threshold of $\Delta E=11.4$ eV, is normalized to unity at $\theta=90^\circ$.

to $\sqrt{3}K_{\min}$, cause peaking along \mathbf{k}_0 and thus oppose the formation of a $\sin^2\theta$ distribution. In the high-energy limit, the integrand of (52) will be dominated by some leading inverse power of K , so that the indefinite integral has the functional form $-\beta K^{-n}$ where, in general, $n \geq 0$. The fraction ξ of the total integral for which $\theta' \leq \theta'_{\text{magic}}$ is thus given by

$$\xi(\theta' \leq \theta'_{\text{magic}}) = \frac{(-\beta K^{-n})_{K_{\min}} \sqrt{3}K_{\min}}{(-\beta K^{-n})_{K_{\min}} K_{\max}} \approx 1 - 3^{-n/2}, \quad (54)$$

which is seen to be independent of the bombardment energy E_0 . It is evident from Table I which lists the values of $\xi(\theta' \leq \theta'_{\text{magic}})$ as a function of n , that with increasing inverse powers of K , the contribution of values of $\theta' \leq \theta'_{\text{magic}}$ to the form of $I(\theta, \phi)$ becomes accentuated. Indeed Table I shows that if the weighting of small-angle scattering is sufficiently pronounced, the angular distribution need not be reversed in sense, even in the limit of high bombarding energies. These conclusions concerning the form of anisotropies in the high-energy limit of the Born approximation are quite

TABLE I. Fractional contribution to the scattering cross section made by those angles for which $\theta' \leq 54.7^\circ$, calculated by Eq. (54) for the high-energy limit.

n	$\xi(\theta' \leq \theta'_{\text{magic}})$
0	0.00
1	0.42
2	0.67
3	0.81
4	0.89

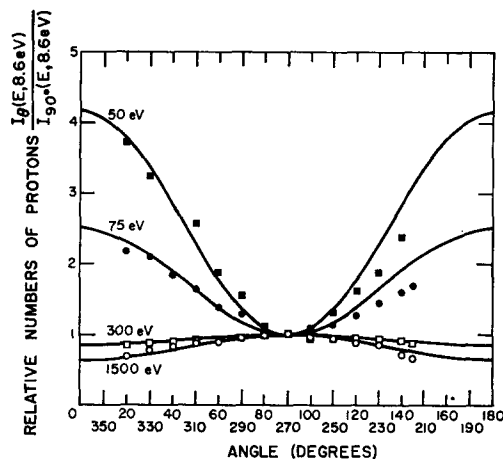


FIG. 8. Angular distribution of 8.6-eV protons for various electron energies formed by the dissociative ionization process $\text{H}_2 + e \rightarrow \text{H} + \text{H}^+ + 2e$. This figure is reproduced from Fig. 3 of Ref. 6 with the kind permission of the authors.

general, but appear to have been overlooked in the literature.³¹

We present in Fig. 8 the angular distribution of "fast" protons measured by Dunn and Kieffer⁶ for the different but closely related problem of the dissociative ionization of H_2 by electron impact. Figures 7 and 8 have much the same qualitative form, showing a nearly cosine-squared distribution at low bombarding energies but deforming with increasing bombarding energy to a limiting distribution in which the form of the anisotropy is only slightly reversed. Rather than comparing values of $I(\theta, \phi)$ at the same corresponding energies E_0 , the agreement between Figs. 7 and 8 is heightened if we compare instead angular distributions at the same multiples of the respective threshold energies of the two figures. When viewed in this manner, the high degree of similarity between Figs. 7 and 8 encourages us to believe that this general calculational procedure is probably applicable to a wide class of dissociative molecular processes, provided a single repulsive potential is chiefly responsible for the observed molecular fragmentation. In the electron impact dissociation of H_2^+ and the dissociative ionization of

³¹ For example, I. C. Percival and M. J. Seaton, *Phil. Trans. Roy. Soc. (London)* **215**, A15 (1958), calculated the degree of polarization P of the radiation emitted in the electron impact excitation of atoms. Close to threshold they found P to be a large positive fraction, while far from threshold they calculated that P would be a large negative fraction, the value depending on the specific transition studied. However, in performing the integration of the scattering cross section over K [see Eqs. (6.13), (6.14), and (6.15) of their paper], they assumed they could replace $\cos\theta'$ by zero in the high-energy limit. This approximation is not justified in general because of the inordinately strong weighting given to small angle scattering caused by the presence of inverse powers of K in the expression for the scattering cross section as a function of K . If the integrand varies as K^{-1} or slower, their conclusions are correct in the limit of high energy, but the approach may be as slow as logarithmic. If the integrand varies more rapidly than K^{-1} , the degree of polarization at high energies will not reach the P 's they have calculated, but will approach a value of P intermediate between the values they report for threshold and in the high-energy limit.

H_2 , there is strong evidence³² that indeed the major source of dissociation fragments is a single repulsive potential curve (the $2p\sigma_u$ $^2\Sigma_u^+$ state of H_2^+). Unfortunately, this need not apply to other molecules where neighboring repulsive curves of different symmetries may vie with each other in the dissociation process,³³ causing the distribution of products to be less anisotropic than we have pictured.

Finally, we wish to discuss the behavior of Figs. 7 and 8 in the limits of large and small electron beam energies. To the extent we can describe the high-energy form of the angular distribution shown in Fig. 7 by an average θ' , we find from the relationship

$$\theta' = \tan^{-1}[2I(\theta=90^\circ)/I(\theta=0^\circ)], \quad (55)$$

a limiting value of $\theta' = 68^\circ$. This value of θ' compares remarkably well with the value of θ' of about 60° estimated by Dunn and Kieffer for the limiting form of their data presented in Fig. 8. This close agreement indicates that the dependence on the momentum transfer for these different dissociative processes must be quite similar in the high-energy limit.

A comparison of the threshold behavior of Figs. 7 and 8 is not possible, since measurements of the dissociative ionization of H_2 were not carried out at such low electron-beam energies. It may appear somewhat unexpected to find in Fig. 7 that our calculations indicate the $\cos^2\theta$ anisotropy masks the contribution to $I(\theta, \phi)$ from the higher-order partial waves ($l > 1$) in the scattering amplitude. However, this result is not surprising, since close to threshold $|K| \simeq |k_0|$, and for a threshold of $\Delta E = 11.4$ eV used in computing the form of Fig. 7, $|K|$ is about $0.9a_0^{-1}$. From Fig. 3 it is evident that for such small values of K the effects of the higher-order terms can barely be distinguished from a $\cos^2\theta$ behavior. However, for a threshold process of about 35 eV, shown in Fig. 8, $|K|$ is about $1.6a_0^{-1}$, and the contribution of the higher-order terms should be detectable. Thus our Born-approximation calculations predict that if the measurements of Dunn and

³² For the dissociative ionization of H_2 , direct evidence for this conclusion is presented in Ref. 25. For the electron-impact dissociation of H_2^+ the same conclusion must also be inferred from the close agreement between the calculations of J. A. Peek in Ref. 4 and the measured absolute cross section reported in G. H. Dunn, B. Van Zyl, and R. N. Zare, *Phys. Rev. Letters* **15**, 610 (1965); G. H. Dunn and B. Van Zyl, *Phys. Rev.* **154**, 40 (1967).

³³ R. N. Zare and D. R. Herschbach, *J. Mol. Spectry.* **15**, 462 (1965), estimated the relative amount of parallel and perpendicular character in electronic transitions of the alkali halides resulting in an excited alkali atom as one of the dissociation products. They find, using a simple charge-transfer model, that the transition strengths are sufficiently comparable that much of the expected anisotropy in the product distribution is likely to be destroyed when the angular distributions resulting from $\Sigma \rightarrow \Sigma$ and $\Sigma \rightarrow \Pi$ transitions are averaged together. This is in agreement with the scanty experimental evidence available—A. C. G. Mitchell, *Z. Physik* **49**, 228 (1928). Recently, L. J. Kieffer and R. J. Van Brunt [*J. Chem. Phys.* **46**, 2728 (1967)] have reported quite small anisotropies in the measured angular distribution of N^+ ions at low electron bombardment energies, and it seems probable that they are observing this cancellation effect due to repulsive potential curves of different symmetries contributing to the form of the distribution.

Kieffer were extended towards threshold, the fragment distribution would not approach a "pure" $\cos^2\theta$ anisotropy, but would resemble rather the angular distribution given in Fig. 3 for the case of $K=1.5a_0^{-1}$. Of course this prediction is predicated on the assumption that the Born approximation remains a valid description in this low-energy range.

So far no such observations have been made confirming the existence of quantum mechanical interference effects in molecular dissociation. Indeed there appears to be presently no unambiguous information on the angular distribution of products in dissociative excitation. Undoubtedly this lack can be attributed in part to the difficulty of detecting and identifying slow neutral particles. However, there are several possibilities which do not suffer from this experimental drawback and may hold promise for future work. For example, associative detachment as well as the dissociation of molecular ions produces charged fragments which are readily detected. Another class of systems also inviting study are those dissociative processes in which one or more of the fragments separate in an electronically excited state. Then detection can be accomplished either by the characteristic radiation of the fragment or by ejection of secondary electrons if the fragment is in a sufficiently energetic metastable state.

ACKNOWLEDGMENT

My sincere thanks go to Dr. Gordon H. Dunn for encouraging this study and for his useful comments and criticisms throughout the course of this work.

APPENDIX: VARIATION OF THE SCATTERING PHASE SHIFT WITH MOLECULAR ROTATION

If the phase shift δ_J for scattering is expressed in increasing powers of Planck's constant, the first two terms in the series are³⁴

$$\delta_J = (J + \frac{1}{2})\pi - \hbar^{-1} \left((2\mu E)^{1/2} r_* - \int_{r_*}^{\infty} \{ [2\mu(E - V(r)) - (J + \frac{1}{2})^2 / r^2]^{1/2} - (2\mu E)^{1/2} \} dr \right), \quad (A1)$$

where E is the energy of the scattered particle, $V(r)$ is the central-field potential and r_* is the value of r for which $E = V(r_*) + (J + \frac{1}{2})^2 / 2\mu r_*^2$ (the classical turning point). The next term of this expansion enters with the power \hbar^{-3} , and expressions for this term and all

³⁴ J. de Boer and R. B. Bird, "Quantum Theory and Transport Phenomena" in *Molecular Theory of Gases and Liquids*, J. O. Hirschfelder, C. F. Curtiss, and R. B. Bird, Eds. (John Wiley & Sons, Inc., New York, 1964), Chap. 10.

higher-order members of this series expansion are given elsewhere.³⁵

We wish to show for large recoil energies that $\delta_J - J\pi/2$ is nearly independent of J . We define the momentum variables $\hbar^2 \kappa^2 = 2\mu[E - V(r)]$ and $\hbar^2 k^2 = 2\mu E$. Then (A1) may be put into the form

$$\delta_J = (J + \frac{1}{2})\pi/2 - kr_* + \int_{r_*}^{\infty} (\kappa \{ 1 - [(J + \frac{1}{2}) / (\kappa r)]^2 \}^{1/2} - k) dr. \quad (A2)$$

By expanding the expression within the braces in (A2), we find that

$$-kr_* + \int_{r_*}^{\infty} (\kappa \{ 1 - [(J + \frac{1}{2}) / (\kappa r)]^2 \}^{1/2} - k) dr \quad (A3)$$

is independent of J to terms of order $[(J + \frac{1}{2}) / (\kappa r)]^2$. This proves the assertion made in the main text in Eq. (35).

Alternatively³⁶ we may differentiate Eq. (A1) with respect to J (bearing in mind that r_* depends on J). We find that

$$\frac{\partial \delta_J}{\partial J} = \frac{1}{2}\pi - \int_{r_*}^{\infty} \frac{(J + \frac{1}{2}) dr}{r^2 [\kappa^2 (J + \frac{1}{2})^2 / r^2]^{1/2}}, \quad (A4)$$

where the right-hand side of (A4) is recognized as one-half the classical deflection angle $\theta/2 = \pi/2 - \chi$. Calculations for χ have been performed previously for the photodissociation of NaI. It was shown that χ was close to zero and insensitive to variation in J for nearly axial recoil.^{3,9}

We might question whether the phase-shift expansion given in (A1) is valid for very small J . Most derivations of the semiclassical phase shift in the past have used the approximation that $J(J+1)$ may be replaced by $(J + \frac{1}{2})^2$ for large J . It has been demonstrated, however, that this additional assumption is not required to derive (A1) and that the factor $(J + \frac{1}{2})$ arises naturally if the appropriate boundary conditions are imposed.³⁵ Furthermore the quantum mechanical phase shifts calculated by Bernstein³⁷ for a Lennard-Jones potential at high energy but small angular momentum shows the behavior described above ($|\delta_{J+1} - \delta_J| = \pi/2$ to 0.1 rad or better) for a wide range of conditions and suggest the general validity of these results for nearly axial recoil.

³⁵ C. F. Curtiss and R. S. Powers, Jr., *J. Chem. Phys.* **40**, 2145 (1964); S. Choi and J. Ross, *ibid.* **40**, 2151 (1964).

³⁶ Reference 34 develops a power-series expansion in \hbar for the difference in the phase shifts $\delta_{J+1} - \delta_{J-1}$ and investigates how in the correspondence limit this approaches the deflection angle χ . See also Ref. 11, Chap. 5, Sec. 5.

³⁷ R. B. Bernstein, *J. Chem. Phys.* **33**, 795 (1960).